Electronic Supplementary Material (ESI) for ChemComm.

Structural effects of oxidation on sugars: Glucose as a precursor of gluconolactone and glucuronolactone

Maider Parra-Santamaria[1, †], Aran Insausti[2, †], Elena R. Alonso[3], Francisco J. Basterretxea[4] and Emilio J. Cocinero[5]

[1,2,3,4,5] *Departamento de Química Física, Facultad de Ciencia y Tecnología, Universidad del País Vasco (UPV/EHU), Campus de Leioa, Ap. 644, 48080 Bilbao, Spain.*
[2] *Instituto Biofisika (CSIC, UPV/EHU), 48080 Bilbao, Spain.*
[3] *Current address, Quifima Building, Parque Cientifico UVa, Universidad de Valladolid, 47005 Valladolid, Spain.*
[†] *These authors contributed the same.*

Corresponding author: Emilio J. Cocinero → emiliojose.cocinero@ehu.eus

Contents

1 Computational Methods

The first step[1] involved an exhaustive conformational search of the system using a molecular mechanics (MM) method that combine advanced Monte Carlo and large-scale low-mode atomic redistribution algorithms. In order to avoid any missing conformation three different force-fields were used: Merck Molecular Force Field (MMFFs)[2], Optimised Potentials for Liquid Simulations (OPLS)[3] and Assisted Model Building with Energy Refinemen (AMBER)[4]. All the geometries found were later fully re-optimised by quantum mechanical methods, such as the MP2[5] *ab initio* method and Density Functional Theory (DFT) based B3LYP-D3BJ[6,7]. In both cases, the basis-set used was the Popple's triple zeta 6-311 basis increased with polarisation and diffusion functions (6-311++G(d,p))[8,9,10]. On the other hand, vibrational contributions in the rotational constants were calculated using the calculated first-order vibration-rotational constants α_i that define the well-known vibrational dependence of rotational constants

$$B_v = B_e - \sum_i \alpha_i(\nu_i + 1/2) \tag{1}$$

where, B_ν and B_e substitute all three rotational constants in a given excited state and in equilibrium, repectively. ν_i is is the vibrational quantum number of the "ith" vibrational mode. The α_i constants of the experimental conformers were obtained from anharmonic calculations at the B3LYP-D3BJ/6-311++G(d,p)[6,7,8,9,10]. All the theoretical calculations were implemented in Gaussian 16.[11]

1.1 Theoretical Conformational Analysis of Gluconolactone (GlcL)

Table S1: Predicted A, B and C rotational constants, dipole moments, relative energies and Gibss free energies for **GlcL** at MP2 level using 6-311++G (d,p) basis.

GlcL	**1**	**2**	**4**	**3**	**5**	**6**	**7**	**8**	**9**
A / MHz	1205.1	1230.2	1216.84	1369.4	1077.7	1276.2	1244.3	1246.3	1373.2
B / MHz	848.1	802.8	845.4	752.7	965.8	811.8	791.4	784.5	761.9
C / MHz	552.2	503.1	557.6	504.3	641.7	539.2	502.2	499.9	508.2
$\lvert\mu_a\rvert$ / D	1	2	2	1	3	0	0	1	6
$\lvert\mu_b\rvert$ / D	1	1	1	3	0	3	2	3	1
$\lvert\mu_c\rvert$ / D	1	1	0	1	2	1	2	0	1
$\Delta E + ZPE$ / kJ·mol^{-1}	0.0	2.6	5.7	6.0	6.2	8.1	12.7	14.3	16.1
ΔG_{298K} / kJ·mol^{-1}	0.0	2.8	4.7	6.8	6.4	8.1	11.7	13.5	16.1

Table S2: Predicted parameters for **GlcL** at B3LYP-D3BJ level using 6-311++G (d,p) basis.

GlcL	**1**	**2**	**3**	**4**	**5**	**6**	**7**	**8**	**9**
A/MHz	1189.9	1224.0	1367.9	1188.7	1071.6	1252.3	1241.4	1242.3	1367.8
B/MHz	845.6	797.0	747.9	848.0	946.0	808.9	783.1	776.8	756.9
C/MHz	551.4	499.7	500.8	562.1	640.6	537.6	498.4	496.2	505.1
$\lvert\mu_a\rvert$ /D	0	2	1	2	3	1	1	1	6
$\lvert\mu_b\rvert$ /D	1	2	3	1	0	3	3	3	1
$\lvert\mu_c\rvert$ /D	0	1	1	0	2	1	2	0	1
$\Delta E + ZPE$ / kJ·mol^{-1}	0.0	2.2	4.5	6.0	6.4	8.1	12.7	13.4	15.1
ΔG / kJ·mol^{-1}	0.0	2.3	5.5	4.2	6.3	7.5	11.8	12.5	15.4

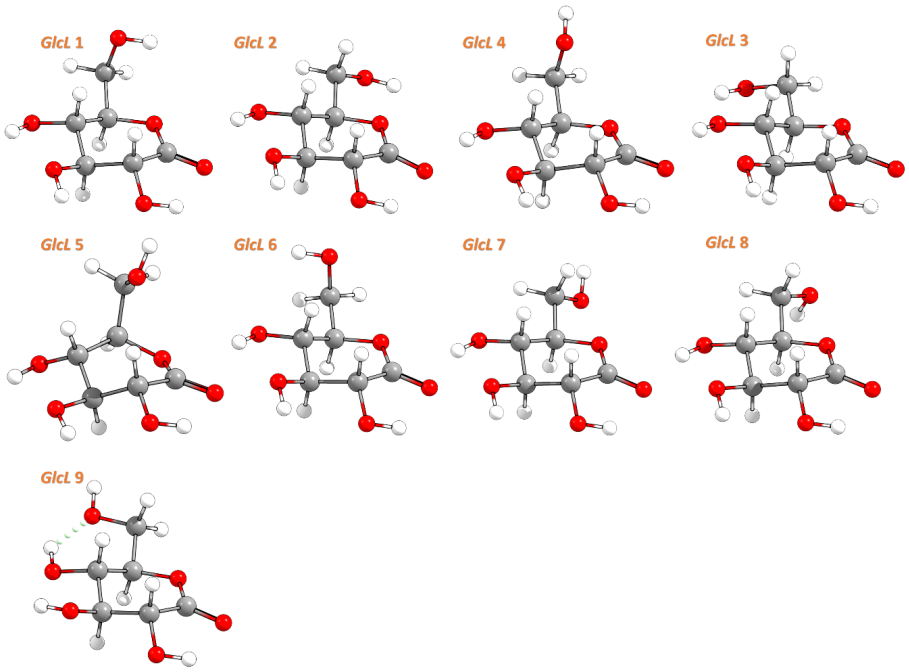

Figure S1: Minima identified for **GlcL** optimised at MP2 level using 6-311++G (d,p) basis.

1.1.1 Nomenclature used for GlcL

The terminology used to name the different conformers **GlcL** has been chosen taking into account the three staggered orientations of the torsional angle ω and the counterclockwise (**cc**)/clockwise (**c**) orientation of the hydroxyl (OH) groups leading to a cooperative network of hydrogen bonds (HBs) as indicated below:

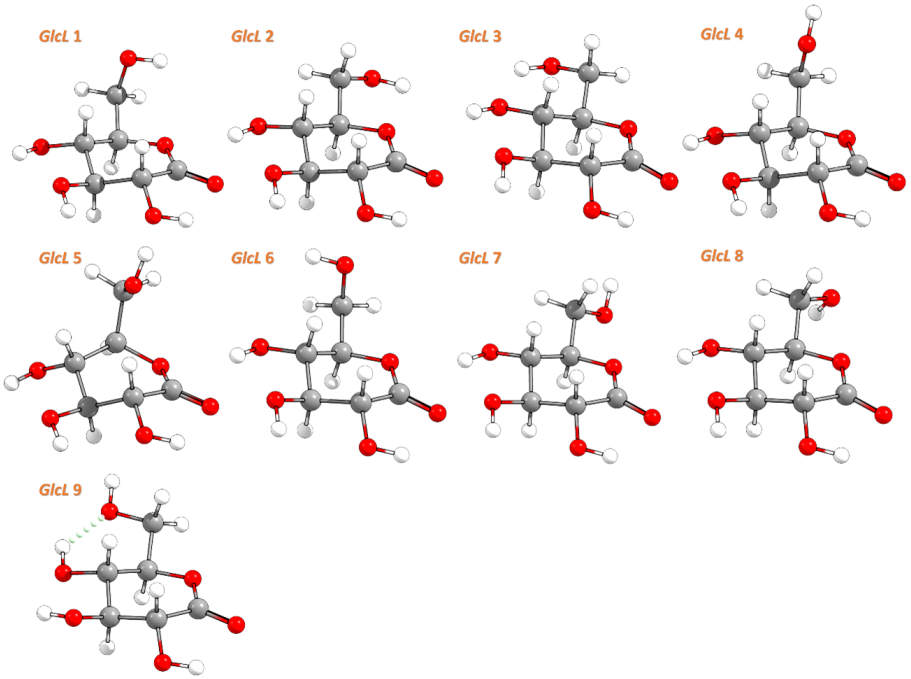

Figure S2: Predicted structures for **GlcL** optimised at B3LYP-D3BJ level using 6-311++G (d,p) basis.

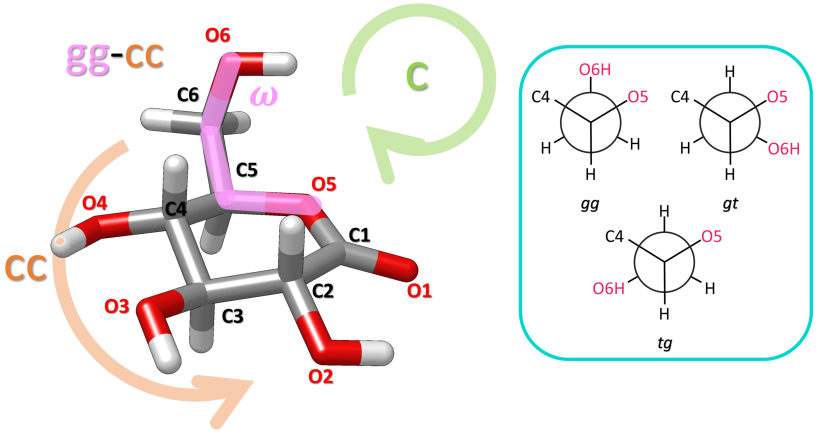

Figure S3: Indication of the torsional angle ω for the molecular system and the nomenclature used according to its value.

1.2 Theoretical Conformational Analysis of Glucuronolactone (GlcurL)

Table S3: Predicted parameters for β-f-GlcurL at MP2 level using 6-311++G (d,p) basis.

β-f-GlcurL	1	2	3	4	5	6	7	8	9	10	11
A/MHz	1669.60	1582.50	1648.90	1654.70	1587.50	1585.10	1590.90	1611.50	1594.10	1540.30	1551.70
B/MHz	884.80	811.10	884.00	880.10	805.60	831.20	831.10	856.30	822.10	858.00	851.80
C/MHz	787.20	774.70	784.20	781.20	771.20	788.60	784.60	791.40	780.80	694.00	692.10
$\lvert\mu_a\rvert$ /D	1	4	2	2	4	5	4	3	3	0	2
$\lvert\mu_b\rvert$ /D	2	1	1	1	1	2	1	3	2	1	0
$\lvert\mu_c\rvert$ /D	2	2	1	2	4	0	2	1	3	0	1
$\Delta E + ZPE$ / kJ·mol^{-1}	0.0	0.7	1.8	2.8	3.2	3.7	3.8	4.7	5.8	19.8	21.6
ΔG / kJ·mol^{-1}	1.1	0.0	2.0	2.5	2.5	1.3	1.7	4.0	5.0	19.3	20.9

Table S4: Predicted parameters for β-f-GlcurL at B3LYP-D3BJ level using 6-311++G (d,p) basis.

β-f-GlcurL	1	2	3	4	5	6	7	8	9	10	11
A/MHz	1647.0	1569.6	1620.0	1626.8	1564.1	1574.6	1570.5	1584.4	1589.2	1514.6	1524.7
B/MHz	873.8	797.6	874.6	869.7	819.8	793.7	821.3	814.2	842.9	860.6	854.6
C/MHz	771.9	772.2	765.7	763.7	770.4	767.4	766.7	775.0	776.8	688.2	686.7
$\lvert\mu_a\rvert$ /D	1.1	4.5	2.2	1.7	5.2	3.8	4.6	3.0	3.7	0.3	-1.3
$\lvert\mu_b\rvert$ /D	1.7	0.6	1.0	-0.9	1.8	-0.4	0.3	1.2	2.8	0.7	-0.5
$\lvert\mu_c\rvert$ /D	-2.7	-2.2	-1.3	-2.2	-0.5	-4.1	-1.9	-2.8	-1.4	-0.5	-0.8
$\Delta E + ZPE$ / kJ·mol^{-1}	0.0	0.1	0.9	2.1	2.2	2.2	2.3	3.6	3.7	11.9	13.4
ΔG / kJ·mol^{-1}	1.1	0.0	1.0	2.0	0.9	1.8	1.2	3.6	3.5	12.1	13.5

*

*α-**GlcurL 5** conformer converged to α-**GlcurL 2** using MP2/6-311++G(d,p).

Table S5: Predicted parameters for α-***f*-GlcurL** at MP2 level using 6-311++G (d,p) basis.

α-f-GlcurL	1	2	3	4	5
A/MHz	1767.0	1812.8	1731.6	1676.3	-
B/MHz	741.5	732.1	744.9	759.2	-
C/MHz	661.2	654.4	670.3	688.4	-
$\lvert\mu_a\rvert$ /D	3.2	1.5	4.3	2.6	-
$\lvert\mu_b\rvert$ /D	1.2	0.5	2.1	0.7	-
$\lvert\mu_c\rvert$ /D	0.3	0.7	2.6	3.7	-
$\Delta E + ZPE$ / kJ·mol^{-1}	0.0	2.2	4.8	13.4	-
ΔG / kJ·mol^{-1}	0.0	2.0	4.2	14.3	-

†

† Only b3lyp calculations were performed for this form, as we did not expect to observe it experimentally.

Table S6: Predicted parameters for α-***f*-GlcurL** at B3LYP-D3BJ level using 6-311++G (d,p) basis.

α-f-GlcurL	1	2	3	4	5
A/MHz	1766.4	1817.9	1725.1	1676.9	1795.8
B/MHz	735.6	723.9	741.4	754.3	760.4
C/MHz	639.1	632.6	651.1	668.3	628.7
$\lvert\mu_a\rvert$ /D	3.6	2.0	4.4	3.0	2.6
$\lvert\mu_b\rvert$ /D	1.5	0.8	2.8	0.8	3.3
$\lvert\mu_c\rvert$ /D	0.4	0.6	3.0	3.9	1.4
$\Delta E + ZPE$ / kJ·mol^{-1}	0.0	1.6	4.2	12.4	16.1
ΔG / kJ·mol^{-1}	0.0	0.8	3.8	13.6	17.0

Table S7: Predicted parameters for β-***p*-GlcurL** at B3LYP-D3BJ level using 6-311++G (d,p) basis.

β-p-GlcurL	1	2	3	4	5	6
A/MHz	1418.8	1405.1	1401.9	1411.9	1405.5	1365.2
B/MHz	1011.7	1029.4	1028.8	1022.8	1014.1	898.2
C/MHz	852.8	838.7	837.7	841.6	840.4	795.5
$\lvert\mu_a\rvert$ /D	1.8	3.4	3.5	2.9	1.8	3.9
$\lvert\mu_b\rvert$ /D	1.0	-0.9	-2.5	2.8	2.4	2.2
$\lvert\mu_c\rvert$ /D	2.1	-0.9	0.2	0.7	-0.2	1.0
$\Delta E + ZPE$ / kJ·mol^{-1}	0.0	3.4	3.9	5.8	10.0	18.0
ΔG / kJ·mol^{-1}	0.0	2.8	3.4	5.3	9.5	12.7

‡

‡Only b3lyp calculations were performed for this form, as we did not expect to observe it experimentally.

Table S8: Predicted parameters for ***α-p-GlcurL*** at B3LYP-D3BJ level using 6-311++G (d,p) basis.

α-*p*-GlcurL	1	2	3	4
A/MHz	1405.0	1440.7	1388.4	1399.3
B/MHz	962.9	936.9	967.4	962.9
C/MHz	802.8	817.0	798.4	802.3
$\lvert\mu_a\rvert$ /D	2.4	1.1	3.3	0.9
$\lvert\mu_b\rvert$ /D	1.1	3.1	2.6	5.7
$\lvert\mu_c\rvert$ /D	0.4	0.2	2.9	0.5
$\Delta E + ZPE$ / kJ·mol^{-1}	0.0	2.1	8.4	9.3
ΔG / kJ·mol^{-1}	0.0	2.8	7.8	9.4

Table S9: Predicted parameters for ***l-GlcurL*** at B3LYP-D3BJ level using 6-311++G (d,p) basis.

l-GlcurL	1	2	3	4	5	6	7	8	9	10	11	12	13
A/MHz	1745.3	1335.4	1680.7	1680.8	1655.3	1655.3	1901.3	1679.5	1574.0	1765.9	1444.8	1686.5	1666.8
B/MHz	649.2	827.4	656.5	656.3	695.6	695.6	613.0	668.0	727.9	657.2	858.7	626.1	690.0
C/MHz	608.4	672.7	573.8	573.8	541.3	541.3	499.5	619.6	537.8	551.7	798.1	580.1	543.4
$\lvert\mu_a\rvert$ /D	1.6	1.4	1.9	1.9	0.3	0.3	0.8	2.4	3.8	3.2	2.7	0.9	0.8
$\lvert\mu_b\rvert$ /D	0.3	3.4	2.8	2.8	0.4	0.4	3.3	1.6	0.6	2.7	1.4	1.3	1.2
$\lvert\mu_c\rvert$ /D	2.0	2.4	2.3	2.3	0.3	0.3	1.7	2.4	1.6	4.2	1.4	1.6	1.6
$\Delta E + ZPE$ / kJ·mol^{-1}	0.0	2.4	3.7	3.7	7.2	7.2	8.6	9.2	9.4	10.1	13.6	16.6	19.2
ΔG / kJ·mol^{-1}	0.0	3.1	2.8	2.8	5.6	5.7	7.7	8.1	9.0	9.0	14.9	13.8	16.8

§

§Only b3lyp calculations were performed for this form, as we did not expect to observe it experimentally.

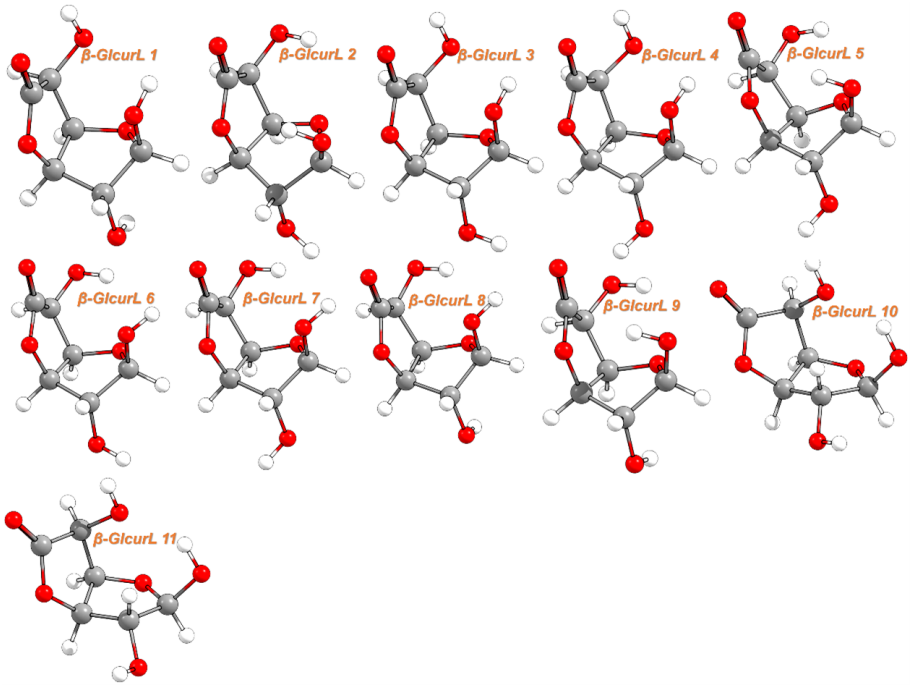

Figure S4: Predicted structures for β-***f*-GlcurL** optimised at MP2 level using 6-311++G (d,p) basis.

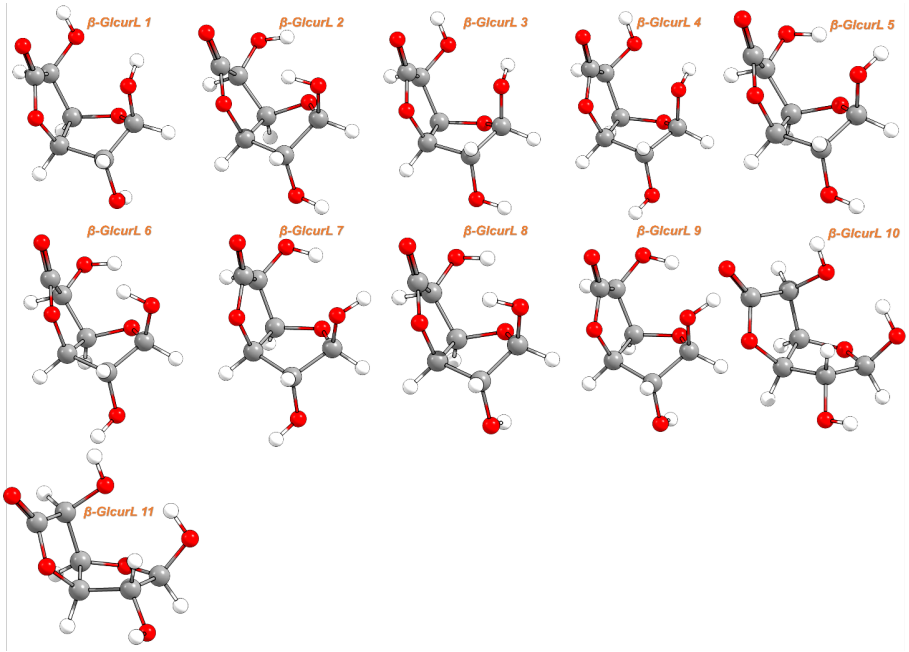

Figure S5: Predicted structures for β-***f*-GlcurL** optimised at B3LYP-D3BJ level using 6-311++G (d,p) basis.

1.2.1 Interconversion barriers

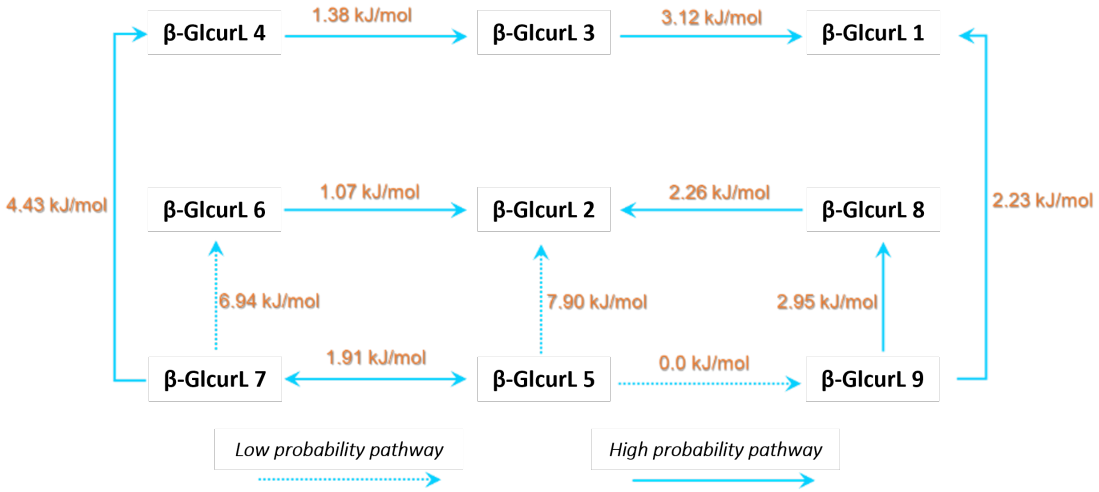

Figure S6: Interconversion pathways among the conformers of β-**GlcurL**.

1.3 NCI Plots

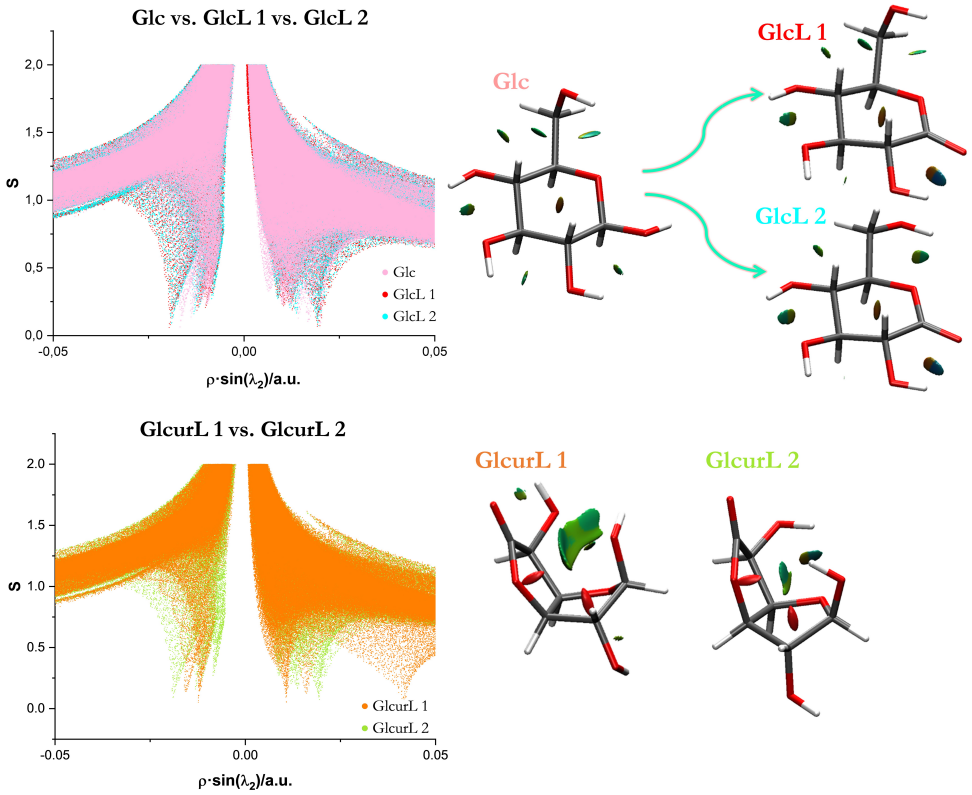

Figure S7: NCI plot for the most stable conformer of β-**Glc** and the experimentally observed conformers of **GlcL** and β-**GlcurL**.

1.4 Cremer-Pople (CP) diagram

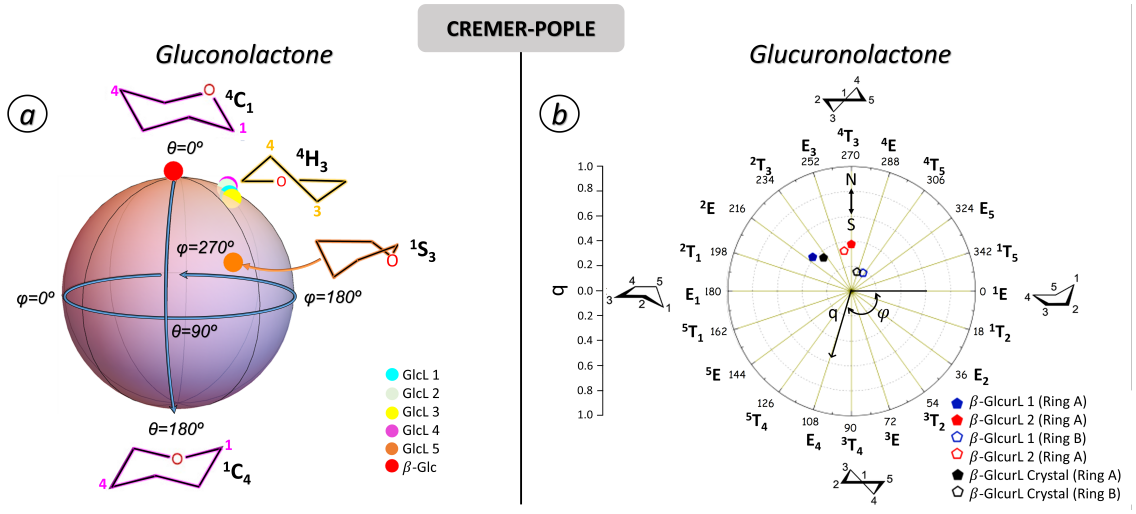

Figure S8: (a) CP-sphere representing the "pure" configurations for six-member pyranose rings together with the six most stable conformers of **GlcL** and β**-Glc**. (b) 2D CP-diagram of the most stable conformers of β**-GlcurL**.

2 Cartesian coordinates for the observed conformers

Table S10: Cartesian coordinates for **GlcL 1**. The geometries have been optimised at the B3LYP-GD3BJ/6-311++G(d,p) level of theory.

Center	Atomic Number	Atomic Type	X	Y	Z
1	8	O	0.436927	1.409941	0.376652
2	6	C	1.217281	0.206645	0.654918
3	6	C	0.661931	-1.043338	-0.022986
4	6	C	-0.837637	-1.135905	0.195822
5	6	C	-1.486862	0.092015	-0.415796
6	6	C	-0.885274	1.383922	0.131044
7	8	O	-1.557530	2.373449	0.262686
8	8	O	-2.879143	0.053849	-0.199777
9	8	O	1.345733	-2.139321	0.562421
10	8	O	-1.281912	-2.334459	-0.423091
11	6	C	2.638543	0.536250	0.222797
12	8	O	2.716447	0.838727	-1.161216
13	1	H	1.190216	0.053038	1.737951
14	1	H	0.863459	-0.997053	-1.100256
15	1	H	-1.053923	-1.165015	1.272712
16	1	H	-1.268819	0.090538	-1.495710
17	1	H	-3.182885	0.969923	-0.121942
18	1	H	0.926345	-2.944451	0.235813
19	1	H	-2.239762	-2.389309	-0.327301
20	1	H	3.263190	-0.340376	0.395767
21	1	H	3.016093	1.364359	0.832715
22	1	H	2.266157	1.678113	-1.306044

Table S11: Cartesian coordinates for **GlcL 1**. The geometries have been optimised at the MP2/6-311++G(d,p) level of theory.

Center	Atomic Number	Atomic Type	X	Y	Z
1	8	O	0.445177	1.421266	0.328941
2	6	C	1.193793	0.218364	0.651790
3	6	C	0.657249	-1.026616	-0.040026
4	6	C	-0.832551	-1.132655	0.198803
5	6	C	-1.492312	0.082838	-0.411372
6	6	C	-0.888590	1.382620	0.111844
7	8	O	-1.565714	2.376886	0.234310
8	8	O	-2.878173	0.032144	-0.155718
9	8	O	1.356414	-2.118143	0.533948
10	8	O	-1.276705	-2.334910	-0.410228
11	6	C	2.628968	0.529230	0.260421
12	8	O	2.738549	0.812310	-1.124324
13	1	H	1.128947	0.066256	1.736265
14	1	H	0.849872	-0.965003	-1.119714
15	1	H	-1.031394	-1.155901	1.281064
16	1	H	-1.298345	0.069936	-1.496304
17	1	H	-3.185265	0.949042	-0.146883
18	1	H	0.904157	-2.912818	0.225263
19	1	H	-2.235762	-2.364475	-0.312491
20	1	H	3.241008	-0.352375	0.458964
21	1	H	2.992351	1.365506	0.869824
22	1	H	2.288390	1.651104	-1.269168

3 Experimental Methods

The MB-FTMW coupled to a laser ablation system at the University of the Basque Country was employed in this work with the objective of obtaining the rotational spectra of both sugar-lactones. The Fourier Transform Microwave spectrometer (FTMW) consists of a Fabry-Pérot resonator where a microwave pulse is guided through two antennas. One of them is fixed to a movable mirror making possible the tuning of all the frequencies in the operating range 4-18 GHz and polarizing the sample previously injected in the vacuum chamber (10^{-7}mmbar) using an inert gas through a solenoid pulse valve.[12,13,14] The subsequent free induced decay is recorded in the time domain and Fourier transformed to the frequency domain. The accuracy of the measurements is better than 3 kHz and rotational transitions separated by more than 10 kHz are resolvable.

The chemicals used are D-(+)-Glucono-1,5-lactone (Gluconolatone, 178.14 g/mol), purchased by TCI, 25g, > 98.0%(T). It appears as a white powder to crystal. Melting point: 153 °C. D-(+)-glucuronolactone (Glucurononolatone, 176.124 g/mol), purchased by xxx, xxx g, xxx > xx%. It appears as a xxx. Melting point: xxx °C.

Approximately 0.7-1 g of the commercial samples were blended with a commercial glue and mechanically compressed into rod forms. These rods were then placed in a stepper motor, rotating, and translating while a homogenous laser beam hits the sample. This laser ablation process, facilitated by a 7-8 mJ (35 ps) third harmonic (355 nm) laser pulse from a Nd:YAG laser, ensures the intact transfer of samples to the gas phase. The vaporized samples were subsequently mixed with the carrier gas, Ar in this instance, at an approximate pressure of 8 bar.

3.1 Relative Populations

As for **GlcL**, an estimation of the relative population of the observed conformers can be obtained by relative intensities (I) measurements. This can be done because there is a direct relation between the intensities and the population of each conformer in the jet (Ar). The relation between them

Table S12: Cartesian coordinates for **GlcL 2**. The geometries have been optimised at the B3LYP-GD3BJ/6-311++G(d,p) level of theory.

Center	Atomic Number	Atomic Type	X	Y	Z
1	8	O	-0.727832	1.199694	0.082660
2	6	C	-1.227452	-0.136002	-0.244279
3	6	C	-0.289272	-1.237534	0.237439
4	6	C	1.121989	-0.950780	-0.249078
5	6	C	1.577114	0.376803	0.330119
6	6	C	0.582436	1.502419	0.050360
7	8	O	0.956424	2.635950	-0.099123
8	8	O	2.856474	0.696645	-0.165839
9	8	O	-0.785791	-2.457222	-0.281697
10	8	O	1.941768	-2.027753	0.182120
11	6	C	-2.613630	-0.211718	0.370268
12	8	O	-3.487249	0.763844	-0.166600
13	1	H	-1.309001	-0.182866	-1.333664
14	1	H	-0.280173	-1.265844	1.337124
15	1	H	1.124804	-0.889947	-1.345699
16	1	H	1.608136	0.275030	1.426934
17	1	H	2.919331	1.662249	-0.198735
18	1	H	-0.098856	-3.122933	-0.152028
19	1	H	2.846186	-1.858085	-0.105703
20	1	H	-2.525592	-0.114916	1.461225
21	1	H	-3.041895	-1.187570	0.142058
22	1	H	-3.099506	1.631773	-0.005678

also includes the values of the dipole moment component involved along each axis (μ_g with g=a,b and/or c) according to the following expression:

$$\frac{N_i}{N_0} \propto \frac{I_i \omega_0 \Delta\nu_i \mu_g(0) \lambda_0 \nu_0^2}{I_0 \omega_i \Delta\nu_0 \mu_g(i) \lambda_i \nu_i^2} \propto \frac{I_i}{I_0} \frac{\mu_g(0)}{\mu_g(i)} \tag{2}$$

where ω is the conformational degeneration and $\Delta\nu$ the line width at half height.[15] In this way, if the transition intensities are well-known for the different conformers, it is possible to estimate the abundance of each conformer respect to the most stable one. The analysis was performed considering nearby in frequency μ_b-type transitions in order to minimise the errors of the estimation, taking into account the MP2 dipole moments values of Table **??**. The average of the data corresponding to a single conformer were used to obtain the final ratio in percentage.

Table S13: Cartesian coordinates for **GlcL 2**. The geometries have been optimised at the MP2/6-311++G(d,p) level of theory.

Center	Atomic Number	Atomic Type	X	Y	Z
1	8	O	-0.739102	1.194740	0.145613
2	6	C	-1.210302	-0.128296	-0.234410
3	6	C	-0.282855	-1.228797	0.256057
4	6	C	1.116384	-0.948363	-0.250038
5	6	C	1.577161	0.374074	0.321697
6	6	C	0.576563	1.498869	0.066971
7	8	O	0.947834	2.638937	-0.083706
8	8	O	2.842007	0.688326	-0.215599
9	8	O	-0.789375	-2.447540	-0.254504
10	8	O	1.942571	-2.022201	0.173043
11	6	C	-2.611280	-0.227433	0.336507
12	8	O	-3.467140	0.759276	-0.208762
13	1	H	-1.260325	-0.157452	-1.329245
14	1	H	-0.266808	-1.243372	1.357423
15	1	H	1.099180	-0.888396	-1.348444
16	1	H	1.637858	0.268858	1.417411
17	1	H	2.915757	1.652138	-0.190493
18	1	H	-0.081197	-3.094707	-0.146391
19	1	H	2.840094	-1.822347	-0.118028
20	1	H	-2.551419	-0.148841	1.431418
21	1	H	-3.030055	-1.199389	0.071384
22	1	H	-3.062340	1.611669	-0.014902

Table S14: Cartesian coordinates for β**-GlcurL 1**. The geometries have been optimised at the B3LYP-GD3BJ/6-311++G(d,p) level of theory.

Center	Atomic Number	Atomic Type	X	Y	Z
1	6	O	1.710752	-0.605656	0.354114
2	6	C	0.622018	-0.955796	-0.680907
3	6	C	0.130297	0.436561	-1.177726
4	6	C	1.293546	0.804164	0.779546
5	1	C	1.723976	-1.314972	1.178305
6	1	C	1.012612	-1.610754	-1.456556
7	1	O	0.329097	0.625410	-2.230201
8	1	O	2.115550	1.414462	1.161281
9	8	O	0.875980	1.404393	-0.439027
10	8	O	2.996150	-0.602568	-0.240887
11	1	C	3.069771	0.167629	-0.817514
12	8	O	-0.495470	-1.621390	-0.057428
13	6	H	-1.576990	-0.815767	0.014050
14	8	H	-2.557973	-1.059559	0.655711
15	6	H	-1.379372	0.406912	-0.880221
16	1	H	-1.910894	0.193176	-1.819260
17	8	H	-1.867697	1.582917	-0.283540
18	1	H	-2.705169	1.350097	0.140704
19	8	H	0.235898	0.695457	1.695419
20	1	H	-0.258697	1.525548	1.676704

Table S15: Cartesian coordinates for β-**GlcurL 1**. The geometries have been optimised at the MP2/6-311++G(d,p) level of theory.

Center	Atomic Number	Atomic Type	X	Y	Z
1	6	O	1.712142	-0.619861	0.331127
2	6	C	0.638590	-0.918944	-0.726346
3	6	C	0.156314	0.500530	-1.144566
4	6	C	1.247126	0.733103	0.857639
5	1	C	1.758716	-1.393727	1.096909
6	1	C	1.039580	-1.524115	-1.540230
7	1	O	0.384248	0.758264	-2.179190
8	1	O	2.038177	1.326715	1.324480
9	8	O	0.872994	1.424335	-0.323786
10	8	O	2.989701	-0.506972	-0.267340
11	1	C	2.989077	0.305024	-0.788571
12	8	O	-0.474342	-1.622110	-0.146479
13	6	H	-1.549803	-0.804061	-0.025507
14	8	H	-2.530958	-1.064000	0.619768
15	6	H	-1.352738	0.441747	-0.883023
16	1	H	-1.861079	0.242029	-1.839352
17	8	H	-1.858989	1.598547	-0.265964
18	1	H	-2.717284	1.342291	0.097535
19	8	H	0.153025	0.518357	1.705829
20	1	H	-0.304275	1.365668	1.786799

Table S16: Cartesian coordinates for β-**GlcurL 2**. The geometries have been optimised at the B3LYP-GD3BJ/6-311++G(d,p) level of theory.

Center	Atomic Number	Atomic Type	X	Y	Z
1	6	O	1.828844	-0.501849	-0.278287
2	6	C	0.557563	-0.352466	-1.101880
3	6	C	0.000370	0.999788	-0.656347
4	6	C	1.432610	0.177722	1.051009
5	1	C	2.107324	-1.548016	-0.126049
6	1	C	0.727473	-0.460579	-2.171830
7	1	O	0.307921	1.837857	-1.280020
8	1	O	2.270466	0.681659	1.533660
9	8	O	0.488069	1.190985	0.680171
10	8	O	2.825724	0.222887	-0.981350
11	1	C	3.650781	0.192551	-0.486805
12	8	O	-0.413045	-1.331673	-0.657068
13	6	H	-1.602638	-0.734657	-0.301951
14	8	H	-2.499679	-1.352781	0.178613
15	6	H	-1.509881	0.772060	-0.605944
16	1	H	-1.943166	0.928644	-1.599743
17	8	H	-2.209747	1.583665	0.286415
18	1	H	-1.709797	1.601627	1.114029
19	8	H	0.919442	-0.705093	2.003551
20	1	H	0.285259	-1.305850	1.591040

Table S17: Cartesian coordinates for β-**GlcurL 2**. The geometries have been optimised at the MP2-GD3BJ/6-311++G(d,p) level of theory.

Center	Atomic Number	Atomic Type	X	Y	Z
1	6	O	1.843613	-0.337939	-0.438097
2	6	C	0.559501	0.040030	-1.152655
3	6	C	0.002400	1.149480	-0.269431
4	6	C	1.427640	-0.215767	1.037904
5	1	C	2.186650	-1.349296	-0.679775
6	1	C	0.705134	0.302054	-2.202431
7	1	O	0.340035	2.151275	-0.540791
8	1	O	2.248616	0.109141	1.681236
9	8	O	0.437308	0.821152	1.056969
10	8	O	2.776431	0.661831	-0.813720
11	1	C	3.592467	0.504380	-0.328178
12	8	O	-0.381361	-1.048635	-1.030143
13	6	H	-1.579245	-0.594381	-0.504446
14	8	H	-2.471139	-1.340495	-0.220373
15	6	H	-1.500655	0.931059	-0.344922
16	1	H	-1.898492	1.384137	-1.261199
17	8	H	-2.243347	1.431210	0.725410
18	1	H	-1.805914	1.117195	1.527455
19	8	H	0.957079	-1.406480	1.589055
20	1	H	0.343506	-1.809337	0.961524

3.2 Experimental data

Table S18: Experimental spectroscopic parameters for the **GlcL** and **GlcurL** rotationally observed conformers.

	GlcL 1	**GlcL 2**	β-***f*-GlcurL 1**	β-***f*-GlcurL 2**
A/MHz	1202.45777(25)	1232.31932(30)	1656.56600(17)	1578.36796 (26)
B/MHz	844.55185(21)	798.73238(19)	874.851218(84)	806.99379 (12)
C/MHz	552.81321(10)	502.244063(77)	782.182652(82)	777.96259 (15)
D_J/kHz	0.02548(93)	0.01085(90)	0.04755(67)	0.05715 (79)
D_{JK}/kHz	—	—	—	—
D_K/kHz	0.1131(66)	—	—	0.1790 (53)
d_1/kHz	-0.00176(48)	-0.00340(69)	0.1285(46)	-0.00810 (69)
d_2//kHz	—	—	-0.00627(35)	—

3.3 Fitted lines

Table S21: Fitted lines and error of β-**GlcurL 1**.

J'	*Ka'*	*Kc'*	←	*J"*	*Ka"*	*Kc"*	ν/MHz	$\Delta\nu$/MHz
4	1	4	←	3	1	3	6428.4163	-0.0014
4	0	4	←	3	0	3	6553.5961	-0.0010
4	2	3	←	3	2	2	6622.0738	0.0004
4	3	2	←	3	3	1	6642.4852	0.0021
4	3	1	←	3	3	0	6644.9176	-0.0013

Table S21 – continued from previous page

J'	Ka'	Kc'	←	J"	Ka"	Kc"	ν/MHz	$\Delta\nu$/MHz
4	2	2	←	3	2	1	6696.5816	-0.0002
5	0	5	←	4	1	3	6761.5777	0.0019
4	1	3	←	3	1	2	6796.6544	0.0014
4	1	4	←	3	0	3	7012.2431	0.0012
3	2	2	←	2	1	1	7316.2330	-0.0026
3	2	1	←	2	1	1	7354.6822	0.0027
3	2	2	←	2	1	2	7594.2400	-0.0009
3	2	1	←	2	1	2	7632.6850	0.0002
5	0	5	←	4	1	4	7685.4135	0.0007
7	1	7	←	6	2	5	7695.9722	-0.0010
4	1	3	←	3	0	3	7936.0769	-0.0020
6	0	6	←	5	1	4	7998.5808	-0.0006
5	1	5	←	4	1	4	8023.5282	0.0001
7	2	5	←	6	3	3	8036.0091	-0.0009
6	1	5	←	5	2	3	8066.3977	0.0020
5	0	5	←	4	0	4	8144.0583	0.0006
5	2	4	←	4	2	3	8267.9087	0.0017
5	3	3	←	4	3	2	8307.7849	0.0003
5	3	2	←	4	3	1	8316.2244	-0.0024
6	1	5	←	5	2	4	8320.2941	0.0000
5	2	3	←	4	2	2	8408.8520	-0.0012
5	1	4	←	4	1	3	8478.4219	0.0003
5	1	5	←	4	0	4	8482.1727	-0.0001
4	2	3	←	3	1	2	8833.2825	0.0012
4	2	2	←	3	1	2	8946.2325	-0.0010
3	3	1	←	2	2	0	9108.2325	-0.0010
3	3	0	←	2	2	0	9108.6425	0.0011
3	3	1	←	2	2	1	9115.9925	-0.0008
3	3	0	←	2	2	1	9116.4025	0.0013
6	0	6	←	5	1	5	9377.3128	0.0007
4	2	3	←	3	1	3	9388.8827	-0.0003
4	2	2	←	3	1	3	9501.8370	0.0017
6	1	6	←	5	1	5	9612.5208	-0.0008
6	0	6	←	5	0	5	9715.4270	-0.0002
7	1	6	←	6	2	4	9728.9978	0.0053
5	1	4	←	4	0	4	9860.9037	0.0003
6	2	5	←	5	2	4	9907.4093	0.0006
8	2	6	←	7	3	4	9930.5766	-0.0036
6	1	6	←	5	0	5	9950.6359	-0.0009
6	3	4	←	5	3	3	9974.3290	0.0018
4	1	4	←	3	1	3	6428.4163	-0.0014
4	0	4	←	3	0	3	6553.5961	-0.0010
4	2	3	←	3	2	2	6622.0738	0.0004
4	3	2	←	3	3	1	6642.4852	0.0021
4	3	1	←	3	3	0	6644.9176	-0.0013
6	3	3	←	5	3	2	9996.4318	-0.0026
9	1	9	←	8	2	7	10114.5030	-0.0012
6	2	4	←	5	2	3	10133.5086	-0.0004
6	1	5	←	5	1	4	10146.4079	0.0000
8	0	8	←	7	1	6	10161.4817	-0.0045
7	1	6	←	6	2	5	10208.9906	-0.0008
5	2	4	←	4	1	3	10304.5357	0.0004
5	2	3	←	4	1	3	10558.4305	-0.0032
4	3	1	←	3	2	1	10751.7827	-0.0001

Table S21 – continued from previous page

J'	*Ka'*	*Kc'*	←	*J"*	*Ka"*	*Kc"*	ν/MHz	$\Delta\nu$/MHz
4	3	2	←	3	2	2	10787.3818	-0.0012
4	3	1	←	3	2	2	10790.2260	-0.0007
7	0	7	←	6	1	6	11039.8892	0.0009
7	1	7	←	6	1	6	11195.7031	-0.0014
5	2	4	←	4	1	4	11228.3726	0.0002
7	0	7	←	6	0	6	11275.1000	0.0021
7	1	7	←	6	0	6	11430.9149	0.0008
7	2	6	←	6	2	5	11539.5361	0.0036
7	3	5	←	6	3	4	11640.8296	-0.0017
7	3	4	←	6	3	3	11689.0533	-0.0012
6	2	5	←	5	1	4	11733.5275	0.0051
7	1	6	←	6	1	5	11796.1084	0.0024
9	2	7	←	8	3	5	11826.0393	-0.0013
7	2	5	←	6	2	4	11861.5089	-0.0013
6	1	5	←	5	0	5	11863.2549	0.0012
8	1	7	←	7	2	6	12092.6435	0.0001
6	2	4	←	5	1	4	12213.5159	-0.0053
5	3	3	←	4	2	2	12360.1397	-0.0023
5	3	2	←	4	2	2	12371.4257	-0.0022
4	4	1	←	3	3	0	12425.4107	-0.0045
4	4	0	←	3	3	0	12425.4351	0.0020
4	4	1	←	3	3	1	12425.8224	-0.0007
4	4	0	←	3	3	1	12425.8466	0.0057
5	3	3	←	4	2	3	12473.0923	-0.0019
5	3	2	←	4	2	3	12484.3783	-0.0018
8	0	8	←	7	1	7	12674.5048	0.0004
8	1	8	←	7	1	7	12773.7943	0.0005
8	0	8	←	7	0	7	12830.3222	0.0015
8	1	8	←	7	0	7	12929.6088	-0.0011
6	2	5	←	5	1	5	13112.2564	0.0034
7	2	6	←	6	1	5	13126.6510	0.0040
8	2	7	←	7	2	6	13163.4637	0.0052
8	3	6	←	7	3	5	13305.6164	0.0004
8	3	5	←	7	3	4	13397.3919	-0.0040
8	1	7	←	7	1	6	13423.1877	0.0033
8	2	6	←	7	2	5	13583.6234	-0.0013
6	3	4	←	5	2	3	13925.6188	0.0028
7	2	5	←	6	1	5	13928.6160	-0.0076
7	1	6	←	6	0	6	13943.9338	0.0015
9	1	8	←	8	2	7	13954.2532	0.0022
6	3	3	←	5	2	3	13959.0069	-0.0023
5	4	2	←	4	3	1	14082.8544	-0.0004
5	4	1	←	4	3	1	14083.0137	-0.0006
5	4	2	←	4	3	2	14085.6982	-0.0002
5	4	1	←	4	3	2	14085.8598	0.0018

Table S22: Fitted lines and error of β-**GlcurL 2**

J'	*Ka'*	*Kc'*	←	*J"*	*Ka"*	*Kc"*	ν/MHz	$\Delta\nu$/MHz
4	1	4	←	3	1	3	6280.1821	0.0001
4	0	4	←	3	0	3	6331.8069	-0.0002
4	2	3	←	3	2	2	6339.1800	0.0003
4	1	3	←	3	1	2	6396.2190	-0.0001

Table S22 – continued from previous page

J'	Ka'	Kc'	←	J"	Ka"	Kc"	ν/MHz	$\Delta\nu$/MHz
3	2	1	←	2	1	1	7072.9910	-0.0036
3	2	2	←	2	1	2	7156.0689	-0.0024
4	1	3	←	3	0	3	7272.7046	-0.0012
5	1	5	←	4	1	4	7848.8051	0.0018
5	0	5	←	4	0	4	7908.8555	-0.0003
5	2	4	←	4	2	3	7922.9604	0.0008
5	4	2	←	4	4	1	7926.5140	0.0025
5	4	1	←	4	4	0	7926.5140	0.0009
5	3	3	←	4	3	2	7927.3592	0.0016
5	3	2	←	4	3	1	7927.6488	-0.0008
5	2	3	←	4	2	2	7938.8579	0.0024
5	1	4	←	4	1	3	7993.6609	0.0017
4	2	2	←	3	1	2	8622.2778	-0.0020
5	1	4	←	4	0	4	8934.5574	-0.0005
6	1	6	←	5	1	5	9416.5475	-0.0009
6	0	6	←	5	0	5	9482.2070	0.0011
6	2	5	←	5	2	4	9506.0642	0.0000
6	5	2	←	5	5	1	9511.6467	0.0006
6	4	3	←	5	4	2	9512.3920	0.0059
6	4	2	←	5	4	1	9512.3920	-0.0012
6	3	4	←	5	3	3	9513.7126	0.0019
6	3	3	←	5	3	2	9514.4904	0.0027
6	2	4	←	5	2	3	9533.5403	0.0001
6	1	5	←	5	1	4	9589.9456	0.0010
5	2	3	←	4	1	3	10164.9112	-0.0048
5	2	4	←	4	1	4	10427.2064	-0.0018
6	1	5	←	5	0	5	10615.6471	0.0005
7	1	7	←	6	1	6	10983.3142	0.0015
7	0	7	←	6	0	6	11051.4847	-0.0010
7	2	6	←	6	2	5	11088.3607	-0.0006
7	5	2	←	6	5	1	11097.4101	0.0021
7	5	3	←	6	5	2	11097.4101	0.0022
7	4	4	←	6	4	3	11098.5655	-0.0037
7	4	3	←	6	4	2	11098.5848	-0.0084
7	3	4	←	6	3	3	11102.1700	0.0008
7	1	6	←	6	1	5	11184.7697	0.0040
6	2	4	←	5	1	4	11704.7952	-0.0017
4	4	0	←	3	3	0	11841.1234	0.0060
4	4	1	←	3	3	1	11841.1354	0.0043
6	2	5	←	5	1	5	12084.4615	-0.0077
7	1	6	←	6	0	6	12318.2085	0.0020
8	1	8	←	7	1	7	12549.0250	0.0006
8	1	8	←	7	1	7	12549.0250	0.0006
8	0	8	←	7	0	7	12616.6314	0.0000
8	2	7	←	7	2	6	12669.7193	-0.0021
8	3	6	←	7	3	5	12687.4734	0.0007
8	3	5	←	7	3	4	12690.9416	0.0001
8	1	7	←	7	1	6	12777.7697	-0.0015
9	1	9	←	8	1	8	14113.6512	0.0036
9	0	9	←	8	0	8	14177.9294	-0.0001
9	2	8	←	8	2	7	14250.0141	-0.0056
9	3	7	←	8	3	6	14274.7823	-0.0007
9	3	6	←	8	3	5	14281.1000	0.0027
9	2	7	←	8	2	6	14336.3793	0.0057

Table S22 – continued from previous page

J'	Ka'	Kc'	$\leftarrow$	J''	Ka''	Kc''	ν/MHz	$\Delta\nu$/MHz
9	1	8	$\leftarrow$	8	1	7	14368.5619	-0.0031

Table S19: Fitted lines and error of **GlcL 1**

J'	*Ka'*	*Kc'*	←	*J"*	*Ka"*	*Kc"*	ν/MHz	$\Delta\nu$/MHz
6	0	6	←	5	1	5	7066.1946	-0.0001
6	1	6	←	5	0	5	7074.0014	0.0000
7	0	7	←	6	1	6	8174.3452	-0.0007
7	1	7	←	6	0	6	8176.3717	-0.0001
8	0	8	←	7	1	7	9280.5206	-0.0015
8	1	8	←	7	0	7	9281.0253	-0.0007
9	0	9	←	8	1	8	10386.1985	-0.0022
9	1	9	←	8	0	8	10386.3232	0.0008
10	0	10	←	9	1	9	11491.7748	0.0036
10	1	10	←	9	0	9	11491.7940	-0.0057
11	0	11	←	10	1	10	12597.3283	0.0035
11	1	11	←	10	0	10	12597.3283	-0.0031
12	0	12	←	11	1	11	13702.8805	0.0012
12	1	12	←	11	0	11	13702.8805	-0.0012
12	1	12	←	11	0	11	13702.8805	-0.0012
4	2	3	←	3	1	2	6226.6789	0.0012
5	2	4	←	4	1	3	7125.0800	0.0002
6	2	5	←	5	1	4	8070.0227	0.0005
7	2	6	←	6	1	5	9095.2470	-0.0007
8	2	7	←	7	1	6	10169.7854	0.0009
9	2	8	←	8	1	7	11264.5921	0.0008
10	2	9	←	9	1	8	12366.4192	0.0015
11	2	10	←	10	1	9	13470.5365	0.0018
5	1	4	←	4	2	3	6553.9182	0.0058
6	1	5	←	5	2	4	7838.1946	0.0019
7	1	6	←	6	2	5	9015.3042	-0.0001
8	1	7	←	7	2	6	10145.0034	-0.0005
9	1	8	←	8	2	7	11257.4379	-0.0002
10	1	9	←	9	2	8	12364.4557	0.0000
6	2	4	←	5	3	3	7862.7479	0.0030
7	2	5	←	6	3	4	9474.8829	-0.0025
8	2	6	←	7	3	5	10853.6964	-0.0057
9	2	7	←	8	3	6	12077.3967	-0.0060
3	3	1	←	2	2	0	6655.5723	-0.0018
4	3	2	←	3	2	1	7836.2223	0.0018
5	3	3	←	4	2	2	8813.1033	0.0018
6	3	4	←	5	2	3	9639.5631	0.0020
7	3	5	←	6	2	4	10417.4181	-0.0022
8	3	6	←	7	2	5	11266.7447	0.0034
9	3	7	←	8	2	6	12232.3379	0.0017
10	3	8	←	9	2	7	13277.7902	0.0013
4	4	1	←	3	3	0	9114.7426	-0.0023
4	4	0	←	3	3	1	9156.5062	-0.0015
4	4	0	←	3	3	0	9122.6153	-0.0038
4	4	1	←	3	3	1	9148.6331	-0.0005
5	5	1	←	4	4	0	11536.5773	-0.0017
5	5	0	←	4	4	1	11546.0972	-0.0013
5	5	0	←	4	4	0	11538.2228	-0.0016
5	5	1	←	4	4	1	11544.4515	-0.0017
6	6	1	←	5	5	0	13945.6354	-0.0002
6	5	1	←	5	4	1	12949.3082	0.0043
6	5	2	←	5	4	2	12997.7206	0.0066

Table S20: Fitted lines and error of **GlcL 2**

J'	*Ka'*	*Kc'*	←	*J"*	*Ka"*	*Kc"*	ν/MHz	$\Delta\nu$/MHz
6	0	6	←	5	1	5	6486.0850	-0.0005
6	1	6	←	5	0	5	6501.1138	0.0013
6	1	6	←	5	1	5	6489.5020	0.0006
6	0	6	←	5	0	5	6497.6964	-0.0002
6	1	6	←	5	0	5	6501.1138	0.0013
7	0	7	←	6	1	6	7495.3973	0.0001
7	1	7	←	6	1	6	7496.3568	-0.0004
7	0	7	←	6	0	6	7498.8114	-0.0016
7	1	7	←	6	0	6	7499.7731	0.0000
8	0	8	←	7	1	7	8501.1784	-0.0032
8	1	8	←	7	1	7	8501.4423	-0.0004
8	0	8	←	7	0	7	8502.1430	0.0013
8	1	8	←	7	0	7	8502.4022	-0.0005
9	0	9	←	8	1	8	9505.9426	-0.0001
9	1	9	←	8	1	8	9506.0120	0.0000
9	0	9	←	8	0	8	9506.2049	0.0010
9	1	9	←	8	0	8	9506.2733	0.0002
6	1	5	←	5	2	4	7247.7438	0.0035
7	1	6	←	6	2	5	8366.0742	0.0014
8	1	7	←	7	2	6	9414.6073	-0.0030
6	1	5	←	5	1	4	7521.0870	0.0020
7	1	6	←	6	1	5	8476.3841	-0.0007
8	1	7	←	7	1	6	9453.9735	-0.0002
9	1	8	←	8	1	7	10446.8545	0.0021
10	1	9	←	9	1	8	11446.5778	-0.0004
11	1	10	←	10	1	9	12448.9865	-0.0006
5	2	4	←	4	1	3	6831.8996	-0.0009
6	2	5	←	5	1	4	7631.3969	-0.0002
7	2	6	←	6	1	5	8515.7479	-0.0004
8	2	7	←	7	1	6	9466.9336	0.0004
9	2	8	←	8	1	7	10450.8848	-0.0012
10	2	9	←	9	1	8	11447.7848	0.0023
4	3	2	←	3	2	1	7859.7478	0.0002
5	3	2	←	4	3	1	7083.8195	0.0011
6	3	3	←	5	3	2	8686.1660	-0.0027

References

[1] C. E. Cleeton and N. H. Williams, *Physical Review*, 1934, **45**, 234.

[2] T. A. Halgren, *J. Comput. Chem.*, 1999, **20**, 720–729.

[3] W. L. Jorgensen, D. S. Maxwell and J. Tirado-Rives, *Journal of the American Chemical Society*, 1996, **118**, 11225–11236.

[4] D. McDonald and W. Still, *Tetrahedron Letters*, 1992, **33**, 7743–7746.

[5] C. Møller and M. S. Plesset, *Phys. Rev.*, 1934, **46**, 618–622.

[6] W. Y. C. Lee and R. G. Parr, *Phys. Rev. B*, 1988, **37**, 785–789.

[7] A. D. Becke, *J. Chem. Phys.*, 1993, **98**, 5648–5652.

[8] A. McLean and G. Chandler, *The Journal of chemical physics*, 1980, **72**, 5639–5648.

[9] T. Clark, J. Chandrasekhar, G. W. Spitznagel and P. V. R. Schleyer, *Journal of Computational Chemistry*, 1983, **4**, 294–301.

[10] R. Krishnan, J. S. Binkley, R. Seeger and J. A. Pople, *The Journal of chemical physics*, 1980, **72**, 650–654.

[11] M. e. Frisch, G. Trucks, H. Schlegel, G. Scuseria, M. Robb, J. Cheeseman, G. Scalmani, V. Barone, G. Petersson, H. Nakatsuji *et al.*, *Gaussian 16, revision C. 01*, 2016.

[12] T. Balle and W. Flygare, *Review of Scientific Instruments*, 1981, **52**, 33–45.

[13] U. Andresen, H. Dreizler, J.-U. Grabow and W. Stahl, *Review of scientific instruments*, 1990, **61**, 3694–3699.

[14] E. J. Cocinero, A. Lesarri, P. Ecija, J.-U. Grabow, J. A. Fernández and F. Castaño, *Physical Chemistry Chemical Physics*, 2010, **12**, 12486–12493.

[15] W. Caminati and J.-U. Grabow, in *Frontiers and advances in molecular spectroscopy*, Elsevier, 2018, pp. 569–598.